

All-metal wakefield accelerator: Two-dimensional periodic surface lattices for charged particle acceleration

I. V. Konoplev^{*}

*JAI, Department of Physics, University of Oxford, Oxford, OX1 3RH, United Kingdom
and Department of Physics, Sevastopol State University, Sevastopol 299053, Russia*



(Received 29 August 2022; accepted 8 November 2022; published 22 November 2022)

Interest in “all-metal” surface periodic structures to control charged particle beam dynamics and properties, and to generate coherent radiation in the THz frequency range has recently risen exponentially. While such structures have the benefits of metal, they are capable of providing similar properties to a dispersive dielectric. All-metal structures allow good temperature and space charge management. Transportation of high energy charge particle beams in the vicinity of the structure without risking material degradation makes them very attractive for particle acceleration and terahertz radiation generation applications. Here, the results of theoretical studies (via numerical modeling) of the electron beam dynamics and wakefield excitation and evolution along the cylindrical two-dimensional periodic surface structure will be presented, and the properties of the wakefields generated will be discussed. The wakefield acceleration of the witness bunch in the potential reaching 1 GV/m will be demonstrated. The challenges will be identified and discussed, and the concept of the cascade accelerator based on such all-metal wakefield accelerator (AMWA) structures will be presented.

DOI: [10.1103/PhysRevAccelBeams.25.111302](https://doi.org/10.1103/PhysRevAccelBeams.25.111302)

I. INTRODUCTION

In recent years, the applications of metal structures with periodic surface perturbations have grown exponentially, especially in the fields of accelerator physics [1–5], high-power sources of coherent radiation [6–11], and particle beam diagnostics [12–15]. One reason for this increasing interest is that the dispersive properties of the structure closely mimic those of a conventional dielectric without the usual drawbacks associated with dielectric materials including vacuum incompatibility; poor temperature and space charge management; and diminished lifetime expectancy under the stress of the harsh radiation environment observed in accelerators and high-power microwave systems. Conventional methods in accelerator physics and vacuum electronics technologies, which have been developed and perfected in the last century, have served to forge new energy frontiers, and enable contemporary research advances in accelerator physics, while also being exploited to produce powerful, intense, coherent radiation at frequencies up to several GHz. Despite these advances, a number of challenges and hurdles, for instance, overcoming rf

breakdown at accelerating gradients above 150 MV/m, remain. Novel concepts and fresh ideas, including the exploitation of newly engineered and functional materials for particle acceleration [1–4,16,17], EM field control [16,18], and high-intensity THz radiation generation [5,19–22] have been studied theoretically and experimentally to maintain the momentum of the scientific progress in these fields. In this paper, using the results observed in previous studies [1–22], we will examine the wakefield excitation by an electron bunch on the surface of a two-dimensional (2D) periodic surface lattice (PSL) of chessboard topology $(-1;0;1)$ [16] [Fig. 1(a)] to enable the acceleration of the witness electron bunch. The numerical model of the periodic surface structure and the electron beams propagating inside has been developed using the 3D Particle-in-Cell (PIC) code, MAGIC. A full outline of the model and a discussion of the wakefield dynamics and properties generated by the beam driver are presented. The acceleration of the witness bunch paired with the driver bunch has been studied, and the results obtained from the 3D PIC model, are presented and discussed. In this paper, the challenges associated with driving beams close to the periodically structured conductive surface are discussed, and the concept of a “cascade” AMWA is introduced. The results of preliminary studies demonstrate that a peak accelerating field up to 1 GV/m can be reached with the average accelerating potential achieved around 300 MV/m allowing the energy of the witness bunch to be boosted from 7 to 10 MeV in a section of 12-mm length.

^{*}Corresponding author’s.
ikonoplev202@gmail.com

Published by the American Physical Society under the terms of the Creative Commons Attribution 4.0 International license. Further distribution of this work must maintain attribution to the author(s) and the published article’s title, journal citation, and DOI.

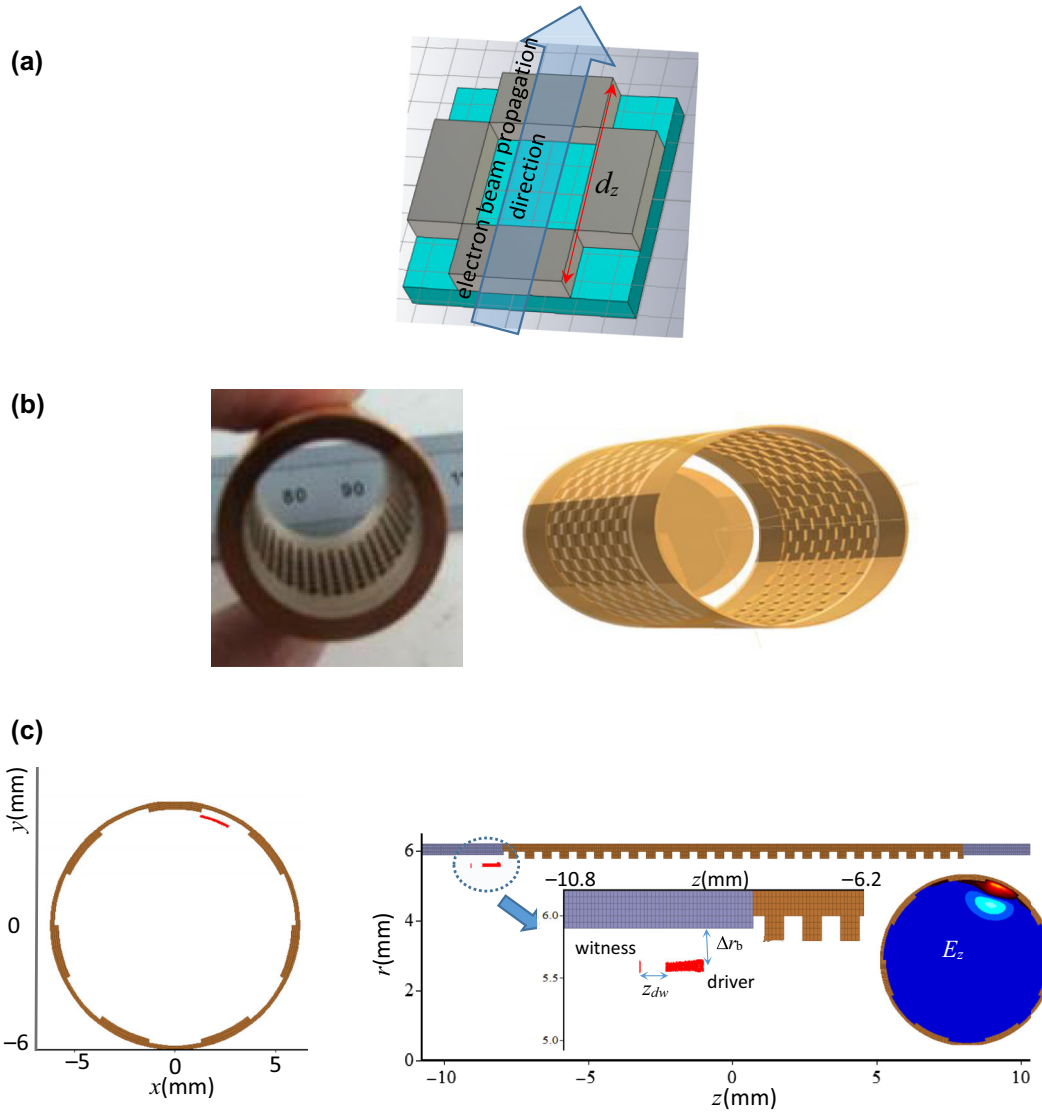


FIG. 1. (a) 3D model basic cell of the 2D periodic surface lattice generated using CST MW Studio with the period of the lattice d_z indicated, (b) photograph (left figure) of the copper, cylindrical, 2D periodic surface lattice, which single cell can be approximated by the “square element” shown in Fig. 1(a), with shallow sine corrugation constructed using 3D printing technique and 3D model (right figure) of the 2D PSL with shallow square wave corrugation build using 3D PiC code MAGIC, with a single cell similar to one shown in Fig. 1(a). Such a structure can be considered as a periodic composition of such elements along azimuthal (\bar{m} periods) and longitudinal coordinates. (c) Numerical model (x, y) and (r, z) views of the periodic structure with driver and witness bunches, the insets on the right figure are zoom-in of the driver and witness bunches and contour plot of the amplitude of the E_z field component in front of the driver bunch.

Conventional dielectric wakefield accelerators are based on waveguides where the radius is comparable to the operating wavelength (usually around several hundred μm) and lined either with continuous or structured dielectric [17,19,23–28]. The waveguide dimensions are typically chosen to allow beam transportation, with minimal beam interception by the dielectric, and to ensure a single mode and high gradient excitation of the wakefield. A compromise must be reached when choosing the diameter of the waveguide, due to the conflicting conditions for lossless beam transportation (for which the electron bunch should be located far from the dielectric) and single mode

excitation (where $r \sim \lambda$). For instance, to get strong interaction, one would bring the charged particle beam as close to the dielectric as possible [17] which may cause partial beam loss due to beam deposition on the dielectric. Most of the dielectrics have poor electric and thermal conductivities and the electric charge deposition may affect the beam transport and the dielectric and mechanical properties of the lining. Moving the beam away from the dielectric lining and increasing the dimensions of the channel will result in a weaker interaction and an increase in the number of higher modes excited in the channel. While the latter, in theory, may be used to control the shape

of the wakefield, it may also lead to challenges with efficient and equal energy transfer from the driver to the different parts of the witness beam, as well as the “side-kicks” which will affect the beam emittance and energy spread. The typical transverse dimensions (diameters) of the dielectric lined wakefield accelerator are several hundreds of micrometers [23–28] while the beam is focused to have dimensions of a few tens of micrometers, i.e., the transverse dimensions of the structures and the beam are comparable. Using small dimensions also means limited power handling capability and thus the limitation of the total accelerated charge.

II. MODEL AND THEORETICAL STUDIES OF WAKEFIELD GENERATION ON 2D ALL-METAL PSL

To overcome the limitations as well as hurdles linked to the properties of the dielectric, using 2D shallow corrugations of the metal surface [Figs. 1(a)–1(c)], i.e., two-dimensional periodic surface lattices (2D PSL) [20–25] are suggested. Here “shallow” means that the amplitude of the corrugation is smaller than one-quarter of the operating wavelength, i.e., avoiding the conventional slow-wave structure configurations. Figure 1(a) illustrates the fundamental cell of the chessboard structure. The fundamental 2D chessboard [Fig. 1(a)] topology [16] can be defined as a superposition of two “waves” $r = r_0 + \Delta r [\cos(\bar{m}\varphi + \bar{k}_z z) + \cos(\bar{m}\varphi - \bar{k}_z z)]$ where Δr is the small amplitude of the corrugations, i.e., $(\Delta r/r_0) \ll 1$ and (φ, z) are the corresponding coordinates in the cylindrical coordinates, while $\bar{k}_z = \frac{2\pi}{d_z}$ is the component of the lattice’s eigenvectors (d_z is the period of corrugation) and \bar{m} is the number of the lattice azimuthal variations. The parameter \bar{k}_z used in the studies has been selected as advised in [20], while taking into account that the goal of the studies, as well as time scales, is significantly different from [20] the parameter \bar{m} has been considered to allow broader (flatter) beam, i.e., the second dimension, $d_m = 2\pi r_0/\bar{m}$, was slightly larger as compared with the beam width. Here, unlike other studies of such structures where the eigenmodes’ formation and evolution toward the steady-state operation have been carried out, the wakefield formation and evolution are considered. The wakefield dynamics occur in a strictly time-dependent regime and the results observed previously [16,20] for instance to define the azimuthal period $d_m = 2\pi r_0/\bar{m}$ ($\bar{m} > 2\pi r_0/\lambda\gamma$, where γ is the relativistic Lorentz factor and λ is the operating wavelength), may not be applicable. The localized wakefield on the 2D surface will be generated immediately and locally by the driver and will dissipate quickly (two or three field oscillations) as soon as the driver moves forward with a velocity close to the speed of light. The expected range of the wavelength excited in the wakefield is defined by d_z while the transverse dimensions and the Q -factor of the localized

wakefields will be defined by d_m and the conductive properties of the material [16].

In Fig. 1(b), photograph of the cylindrical copper structure and 3D model generated by 3D PiC code MAGIC are shown. Such structures with sinusoidal corrugation (left figure) can be studied using a numerical model with the square wave approximation (right figure) due to the small amplitude of the corrugation. In the work presented in this paper, the cylindrical structure [Fig. 1(b)] has been chosen to accommodate intense electromagnetic fields and facilitate electron beam transportation [Fig. 1(c)]. In Fig. 1(c), the (x, y) and (r, z) views (left and right figures, respectively) of the numerical model studied are shown. The red “clusters” near the walls indicate the driver (front) and witness (following) bunches. The insets show the zoom of the driver and witness bunches prior to the entry of the periodic structure, the left figure, the contour plot, (x, y) view, the E_z field component amplitude at the front of the driver beam, and the right figure. In the figures and the left inset, one notes that the clusters consist of microparticles [29] and each microparticle is made of 1000 electrons. Specifically, in these studies, approximately 60,000 microparticles were used to simulate both bunches. To avoid excitation of numerical instabilities, the 3D mesh has been constantly and continuously varied, with a maximum deviation from its mean value by $\sim 30\%$. The mean values of the mesh have been calculated to be equal or less as compared with 1/10 of the expected operating wavelength [10,16].

In previous studies [1–4,30–34], different topologies of the 2D periodic structures were considered and it is understood that chessboard configuration allows minimizing [31] the transverse dispersion of the wakefield, i.e., localizing the wakefield without using small diameter capillary structures [[1–4,17,19,23–26]] and thus maximizing the efficiency [3,19,35] of the energy transfer between driver and witness bunches without compromising beam transport. It allows avoiding the use of dielectric [32,33], as in conventional metamaterials, improving thermal and mechanical properties and thus longevity of the system. The chessboard surface structures can be machined relatively easily with dimensions from several millimeters to several micrometers using different methods including direct machining, electrochemistry, 3D printing, or laser machining [36–38]. One notes that the typical tolerances for the periodic structure dimensions should be better than a tenth of the value of either a specific dimension or the operating wavelength (the smallest is appropriate). One will also need to consider a correct low-loss material if the amplitude (Δr) of the corrugation is very shallow ($\Delta r/r_0 \ll 1$, i.e., the wave coupling parameter is low [38].

In this work, the propagation of the electron bunches off-center of the cylindrical waveguide and in the vicinity of the periodic structure will be studied and the evolution of the bunches will be presented [Fig. 1(c)]. To study the

wakefield excitation, the distance between the driver and the periodic surface will be varied [Fig. 1(c)]. In both cases, namely a single electron bunch (driver) and two-electron bunches (driver and witness, $\gamma_d \neq \gamma_w$), propagation will be considered with the aim of studying the witness bunch acceleration. Thus, the dependence of the witness bunch acceleration on the distance between driver and witness z_{dw} as well as on witness bunch charge and length will be investigated.

Let us assume that the driver propagates near the 2D corrugation (periodic surface lattice, PSL) machined on the inner surface of the hollow metal cylinder [Figs. 1(b) and 1(c)], where it excites a full set of the eigenmodes, providing the resonance conditions are satisfied:

$$\bar{m} = m_v + m_s, \quad \bar{k} = \bar{k}_s - \bar{k}_v$$

where $m_{v,s}$ is the number of azimuthal variations of the volume and surface modes, $\bar{k}_{v,s}$ are the volume and surface wave vectors, and the synchronism condition is

$$\omega = k_z v_z + n\Omega_d,$$

where $\Omega_d = 2\pi v_z/d_z$, n is the harmonic number, and v_z is the longitudinal beam velocity. The geometrical parameters of the lattice (specifically the amplitude and period of the corrugation which both are small in comparison to the wavelength) allow the following two approximations to be made: (1) simplification of the sinusoidal corrugation to a square wave corrugation and (2) description of the structure in terms of an “effective metadielectric” lining on the surface of an unperturbed metal waveguide of radius, r_0 . The inner radius of the effective metadielectric is smaller than the minimum radius of the 2D periodic surface structure corrugation [16] and thus the surface field extends beyond the corrugation’s boundary. As a result, the electron beam can efficiently excite the wakefields without intersecting the structure and the wakefield can be described in terms of the surface currents induced on the metal [5,6,12,16,20,21]. The field excited, as in a dielectric-lined waveguide, will have both longitudinal electric and magnetic field components, E_z and H_z , for which the transverse structure inside the “dielectric,” i.e., close to the 2D PSL, can be defined as [16]:

$$\begin{aligned} E_z &= C_1 [(J_{\bar{m}}(k_{\perp}^s r) Y_{\bar{m}}(k_{\perp}^s r_w) \\ &\quad - Y_{\bar{m}}(k_{\perp}^s r) J_{\bar{m}}(k_{\perp}^s r_w))] \sin(\bar{m}\varphi) \exp(i\bar{k}_z z) \\ H_z &= C_2 [(J_{\bar{m}}(k_{\perp}^s r) Y'_{\bar{m}}(k_{\perp}^s r_w) \\ &\quad - Y'_{\bar{m}}(k_{\perp}^s r) J'_{\bar{m}}(k_{\perp}^s r_w))] \cos(\bar{m}\varphi) \exp(i\bar{k}_z z) \end{aligned} \quad (1a)$$

and outside the dielectric

$$\begin{aligned} E_z &= -(k_{\perp}^s)^2 C_3 [I_{\bar{m}}(k_{\perp}^s r)] \sin(\bar{m}\varphi) \exp(i\bar{k}_z z) \\ H_z &= -(k_{\perp}^s)^2 C_4 [I_{\bar{m}}(k_{\perp}^s r)] \cos(\bar{m}\varphi) \exp(i\bar{k}_z z), \end{aligned} \quad (1b)$$

where C_i are constants. The radial decay of the waveguide surface field toward the center is described using modified Bessel functions $I_{\bar{m}}(k_{\perp}^s r)$ and the imaginary transverse wavenumber of the surface field is $k_{\perp}^s = \sqrt{\bar{k}_z^2 - k^2}$, $Y_{\bar{m}}$ is the Bessel function of the second kind which must be considered for the field defined in the layer away from the center of the structure. The beam width is considerably smaller than the azimuthal period, d_m and the transverse dimension of the localized field is limited by d_m . The wakefield excited will be a superposition of the set of the eigenfields (1) with different azimuthal indices \bar{m} . Such a nonuniform distribution of the wakefield will lead to a high gradient or pondermotive force which will push the bunch from the high field intensity area $\vec{F} = -\vec{\nabla}U(r) = -(\frac{e^2}{4m_0\omega^2})\vec{\nabla}(\frac{E(r)^2}{\gamma(r)})$ creating a significant challenge for high gradient structures. A similar phenomenon observed in planar waveguides lined with a dielectric (DWA structure) has been recently reported in [39]. This phenomenon can affect the acceleration and beam quality and it will be studied using the numerical model in the following section.

III. ALL-METAL WAKEFIELD ACCELERATION–NUMERICAL STUDIES

A. Wakefield formation

In this work, the numerical models developed to study both the beam dynamics and wakefield evolution were created using the 3D PiC code MAGIC3D. Numerical results showing the single bunch dynamics through the structure are shown in Fig. 2(a). A single bunch of total charge, 10 nC, and single particle energy, 7 MeV, has been considered. The effect of the potential depression is relatively strong (for a beam possessing a large charge) and manifests itself as a small perturbation at the head of the beam, as shown in Fig. 2(b). Initially, a monoenergetic beam [blue strip in Figs. 2(a) and 2(b)] has been launched through the uniform cylindrical waveguide of unperturbed radius, $r_0 = 6$ mm. The beam (with no applied magnetic field) travels a length of 1.5 cm along the uniform structure. Due to potential depression, the bunch undergoes a spread in energy prior to entering the 2D periodic structure with an axial period, $d_z = 0.6$ mm. One notes that the driver bunch parameters, such as width, energy, and charge, were maintained constant.

To study the evolution of the wakefield and driver, the beam was propagated through the relatively long structure of length 24 mm, i.e., $L = 40d_z$ while the length of the driver was approximately 0.6 mm (2 ps) with an initial radial thickness of 0.1 mm. Figures 2(a) and 2(b) show the beam energy distributions and evolutions in the cross

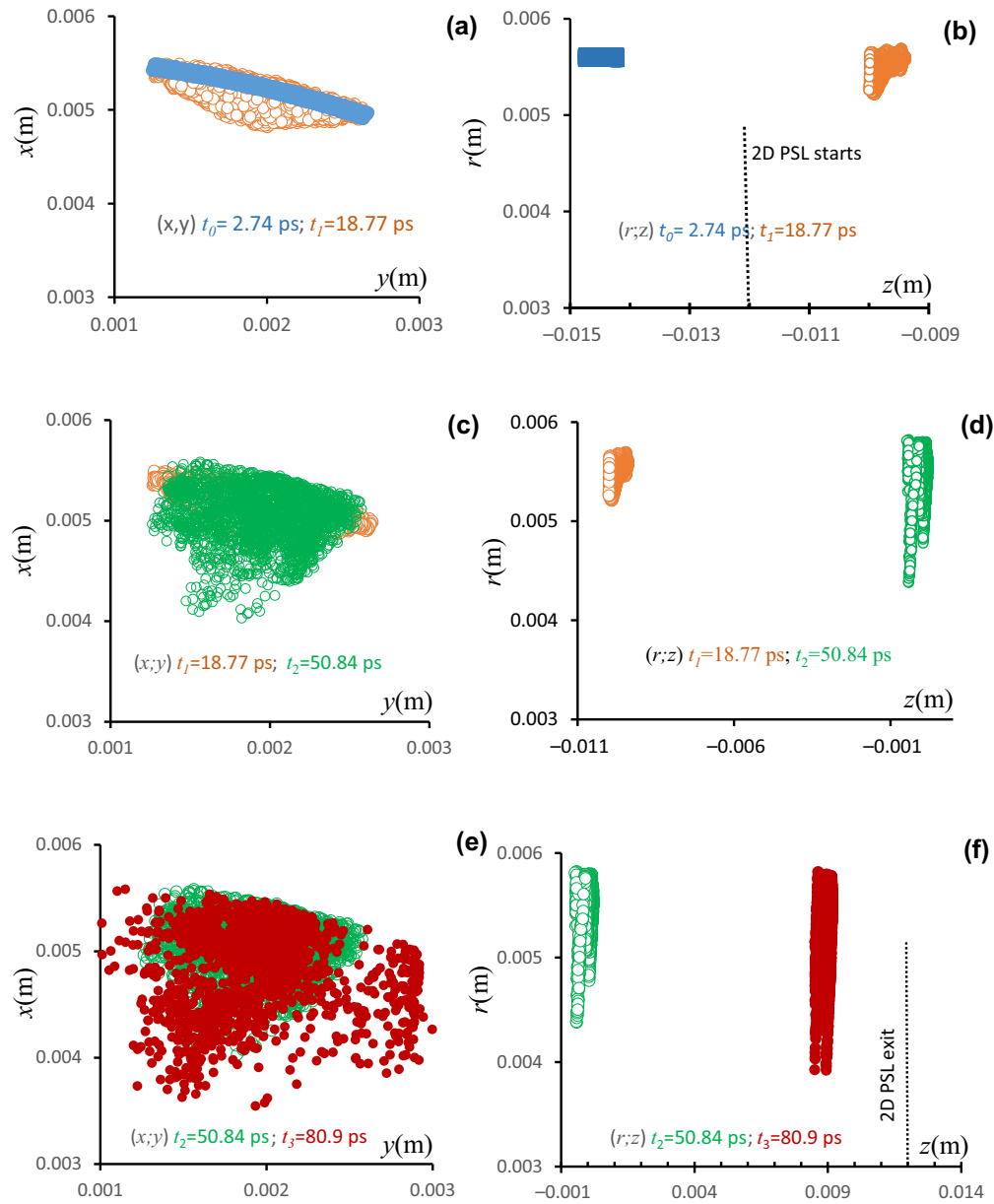


FIG. 2. Results of numerical studies using 3D PiC code MAGIC. Distributions of the electrons inside the driver bunch in (x, y) (first column) and (r, z) cross sections measured at different moments of times (a) and (b) 2.74 (solid blue dots) and 18.77 ps (hollow orange dots); (c) and (d) 18.77 (hollow orange dots) and 50.84 ps (hollow green dots); (e) and (f) 50.84 (hollow green dots) and 80.9 ps (solid red dots). The 2.74 and 80.9 ps are corresponding to injection in and exit from the AMWA structure, while dashed lines in Figs. 2(b) and 2(f) show the entrance and exit of the AMWA.

sections (r, φ) —right column, and (r, z) —left column at several time intervals: (i) 2.74 ps (entry into the structure), (ii) 18.77 ps (first half of the structure) before the beam is pushed to the wall, (iii) 50.84 ps (second half of the structure), and (iv) 80.9 ps (the remains of the beam are deposited in the structure). Each figure shows two distributions of the electrons to better illustrate the evolution of the beam. The beam [Fig. 1(c)] is initially narrow in radial extent (0.1 mm) before it is radially spread by the pondermotive force. This is similar to the effect observed in

laser-plasma interactions where electrons are pushed away from the high intensity laser field creating a bubble. The pondermotive force leads to the exhaustion of the driver, and the dependence of the normalized charge depletion rate on the charge radial position with respect to the grating is shown in Fig. 3(a).

Figure 3(b) illustrates the results of the studies of the dependence of the wakefield amplitude, excitation, and evolution on the radial distance Δr_b [inset to Fig. 1(c)] between the electron beam and PSL (beam PSL

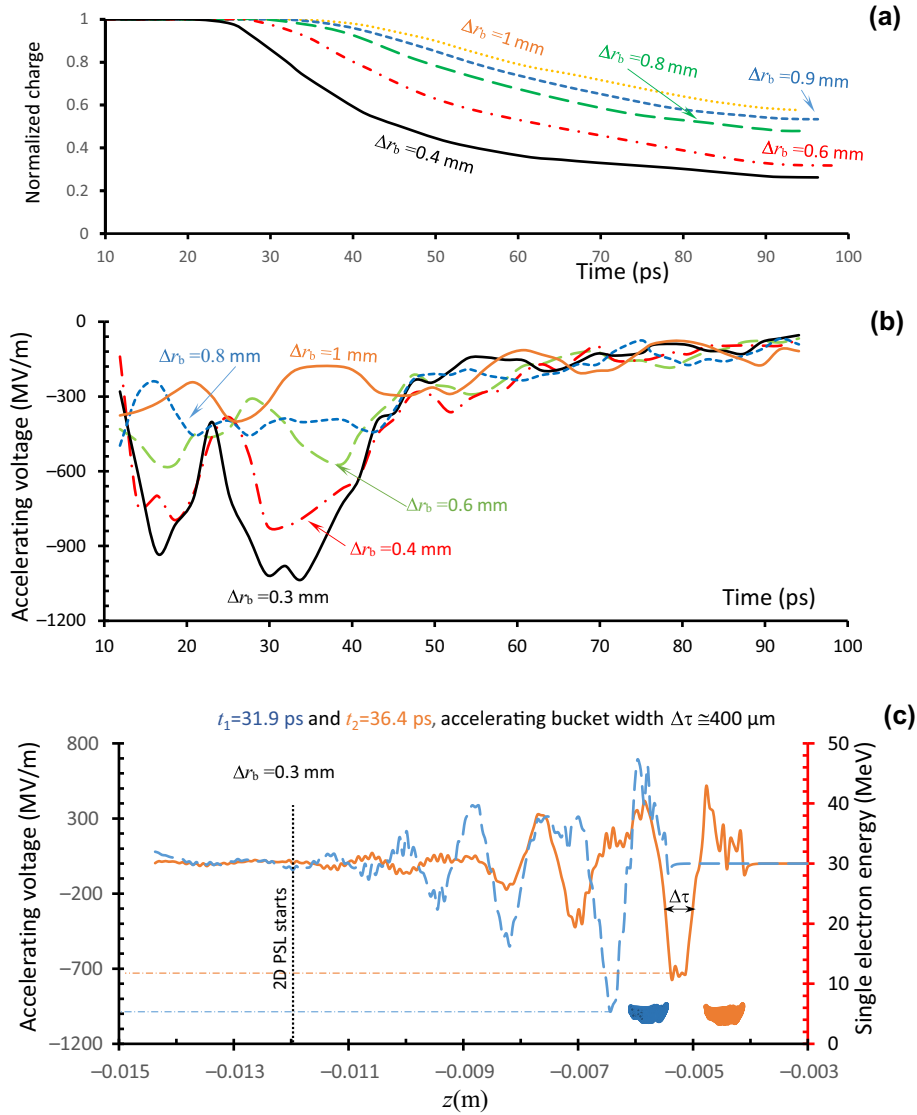


FIG. 3. Results of the numerical studies using 3D PiC code MAGIC. The time dependences of the wakefield driver bunch depletion (a) and the amplitude of the wakefield (b) as the electron bunches propagate through the structure. The results observed for different values of the bunch grating separations $\Delta r_b = 1$ mm (dotted line); $\Delta r_b = 0.9$ mm (short-dashed line); $\Delta r_b = 0.8$ mm (dashed line); $\Delta r_b = 0.6$ mm (dash-dotted line); $\Delta r_b = 0.4$ mm (solid line). The graphs in Figs. 3(a) and 3(b) are observed for the same bunches and illustrate the wakefield amplitude drops in all cases at approximately 50 ps indicating that electron loss and radial dispersion of the bunch are responsible for the amplitude decay. (c) The dependence of the amplitude of the E_z field component of the wakefield inside the periodic structure [waveform (left axis)] taken at two different times $t_1 = 31.9$ ps (dashed blue line) and $t_2 = 36.4$ ps (solid orange line) induced by the high intensity (20 nC, 2 ps, injected bunch CM energy 7 MeV) electron bunch which positions at different times, in respect to the wakefield, are also shown (solid blue/orange dots). The electron energy distribution shown on the right axis of the figure.

separation), the distance between the corrugation (unperturbed radius r_0) and the driver (center of the bunch) was varied from 0.2 to 1 mm. As expected, the depletion of the charge [Fig. 3(a)] leads to the decay of the wakefield accelerating potential as illustrated in Fig. 3(b). Beyond a certain threshold, increasing the length of the corrugation surface will no longer lead to the witness beam acceleration due to the exhaustion of the driver. Figures 3(a) and 3(b) also show that changing the radial position of the beam

with respect to the PSL (i.e., increasing the distance) leads to a decrease in the average accelerating gradient, which then becomes more “monotonic.” One also notes that for a beam-grating separation of 1 mm, the accelerating potential of 1 GV/m has been observed for a significant distance. Moreover, the dip in the accelerating potential observed at the time interval between 20 and 30 ps occurs for all beam positions and is most pronounced for the case where the beam is closest to the surface. Taking these results into

account, we can speculate that this dip is due to interference of the wakes excited at different cells of the PSL structure. As the beam moves away from the structure, the wakefield is less “monochromatic” and has more spectral components of the same amplitude leading to a shallower dip in the accelerating potential. Figure 3(c) shows a typical wakefield waveform for the case where the beam propagates near the surface (1-mm distance) and prior to the bunch depletion. This shows the “regular” sinelike wakefield forms at two-time points: (i) 31.9 and (ii) 34.9 ps which correspond to the case where the bunch is positioned near the center of the 2D PSL. The time interval $\Delta\tau$ indicates the width of the accelerating bucket, $\Delta\tau \cong 1$ ps, and shows that even when the bunch depletion (charge and energy) is weak, the amplitude of the wakefield oscillates as it propagates through the structure. The position of the driver and energy distribution of the particles are also shown for both cases. In the case of the relativistic electron beam with finite $\delta\gamma$ energy spread, the velocity range δv_z is defined as $\delta v_z \sim \delta\gamma/\gamma^3$ explaining the relatively low sensitivity of the synchronism condition $\omega = k_z v_z + n\Omega_d$ to the driver degradation with time and the continuation of excitation of the quasimonochromatic field. It has been observed that the wakefield amplitude decay is more sensitive to the spatial spread of the driver and charge loss rather than to energy spread. As a result, the beam focusing mechanisms needed to overcome the pondermotive force will be beneficial to avoid early exhaustion of the driver bunch.

B. Witness bunch wakefield acceleration

The results of the wakefield studies have enabled the driver-witness bunch pair (DW pair) to be constructed in such a way as to observe the witness bunch acceleration. The results indicate that effective deceleration (radiation generation) of the witness bunch can also be observed by locating the witness bunch within the deceleration phase of the wakefield [Fig. 3(c)]. Accurately positioning the witness bunch into the accelerating potential (negative field) leads to acceleration as shown in Fig. 4(a).

Initial DW-pair studies have been carried out with the 0.1-nC witness bunch (0.6 ps duration) positioned behind the 2-ps long, 8-nC driver at several time intervals. The initial DW pair of the bunches with the single-particle energy of 7 MeV has been launched from some distance (10 mm) from the structure. The DW-pair separation, i.e., the interval between bunches varied from 0.8 to 4 ps. The length of the corrugated structure has been shortened from 24 to 12 mm to minimize the effect of the driver depletion on the witness bunch acceleration (such studies are outside the scope of this paper). The radial thickness of the bunches at the injection point was 0.1 mm and the corrugation depth was 0.16 mm. The radial distance between the center of the

bunches and the unperturbed surface (at the injection point) of the structure was 0.3 mm.

Figure 4(a) illustrates the dependence of the witness bunch’s final energies if the DW-pair separations were 0.8 (dashed lines) and 1.35 ps (solid lines). The lines show the center-mass (CM) energy (center lines), and maximum and minimum single electron energies observed (top and bottom lines), respectively. The inset illustrates the dependence of CM final energy dependence on DW-pair separation, showing that with the large separation, the witness bunch shifts into decelerating phase leading to the deceleration of the bunch. Figure 4(b) shows DW-pair separation at the “intermediate” state at 3.5 ps (dashed lines) with CM energies near the same as the injected energy of the bunch and if the witness bunch is shifted into decelerating phase at 4 ps (solid lines). The inset to Fig. 4(b) illustrates the maximum, CM, and minimum energies observed in the witness bunch as a function of the bunch length. One sees that initially, energy spread grows with the growth of the bunch, and with reaching some length value, the “saturation” of the energy spread is observed. This can be explained by the electron trapping and long bunch microbunching observed and demonstrated in Fig. 4(c). Figure 4(c) illustrates the energy distributions of short (0.05 ps, red dots) and long (1.25 ps, blue dots) electron bunches at the exit from the acceleration section (periodic structure). The microbunching of the long pulse, also seen in the case of the long driver (Fig. 2), “limits” the energy spread which would otherwise be expected to increase as the length of the witness bunch is made longer. For the short-length witness bunch, no microbunching and a reduced energy spread were observed. While the energy spread depends on both the longitudinal and transverse dimensions of the witness bunch in this study, only the longitudinal dimension has been changed. Therefore, taking the following steps such as, minimizing the lengths of both the witness and driver bunches, minimizing the witness bunch radial thickness, and making the wakefield amplitude radial gradient smaller, will help to reduce the energy spread (Fig. 4) while also maximizing the CM energy of the witness bunch.

One notes that addressing challenges associated with driver bunch charge depletion and witness bunch energy spread will be the key goals if the multistage wakefield accelerator is to be constructed. The schematic of such an accelerator is shown in Fig. 5(a). The application of the oversized structure for wakefield acceleration may simplify the overall design of the cascade system. Figure 5(a) shows AMWA sections (squares) based on 2D periodic structures, conditioning systems (arrows) to reduce the energy spread after the AMWA sections, and driver injection and extraction to/from each AMWA section. Figure 5(b) illustrates the change of the beam energy from 7 to 15 MeV (doubling energy) in three sections with the length of the accelerating sections less than 40 mm. The results were obtained under

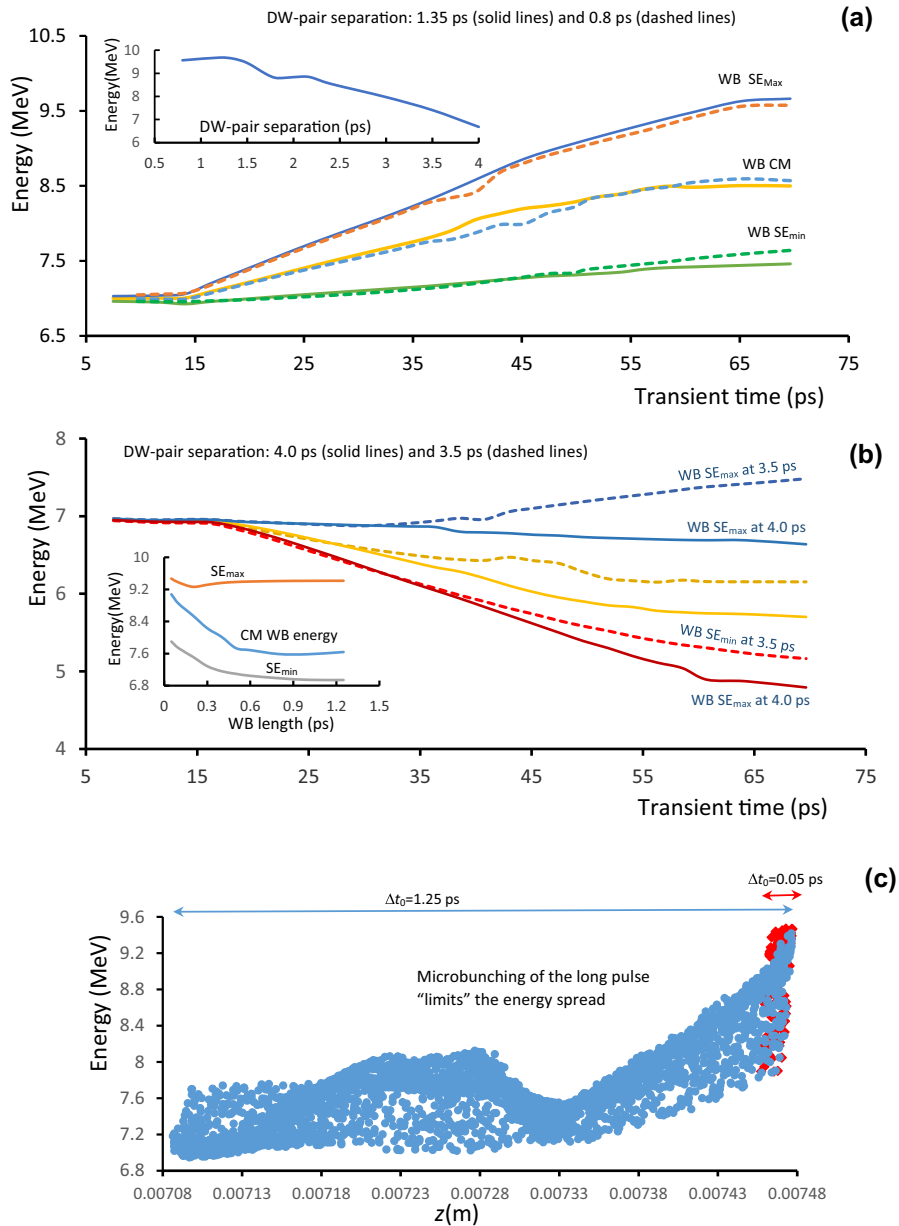


FIG. 4. Results of numerical studies using 3D PiC code MAGIC. Dependences of the witness bunch (WB) energies: (top lines) maximum (max.) single electron (SE_{max}); (middle lines) CM; (bottom lines) minimum (min.) single electron (SE_{min}) on the witness bunch transient through the structure time. The results observed for DW-pair separations (a) 1.35 (solid lines) and 0.8 ps (dashed lines) and (b) 3.5 (dashed lines) and 4.0 ps (solid lines). The inset to (a) shows the dependence of the single electron maximum energy in the witness bunch on the DW-pair separation. The inset to (b) shows WB energies as functions of the WB length: (top line) SE_{max} maximum energy; (middle line) CM; SE_{min} minimum energy (c) illustration of the WB electron density and energy distributions for long (1.25 ps, blue dots) and short (0.05 ps, red dots) at the exit from AMWA structure of 12-mm length.

the assumption that electron beams (at 7, 9, and 12 MeV) with 1% energy spread (typically obtained after conditioning, including collimation) are injected into the accelerating sections. The other properties of the driver and witness bunches are maintained the same as discussed above, i.e., the witness (~ 0.1 nc) and driver (~ 8 nc) bunch lengths were 0.05 and 2 ps, respectively, and the initial DW-pair separation was 1.35 ps. Figure 5(b) illustrates that the energy spread at the exit from the AMWA section does not

depend on the witness bunch's initial energy and the $\Delta E/E_{final}$ is getting smaller with the increase of energy of the injected bunch.

IV. CONCLUSION

In this paper, investigations of the wakefield formation and evolution, excited by the driver (high charge and low energy electron bunch), on the surface of a cylindrical 2D

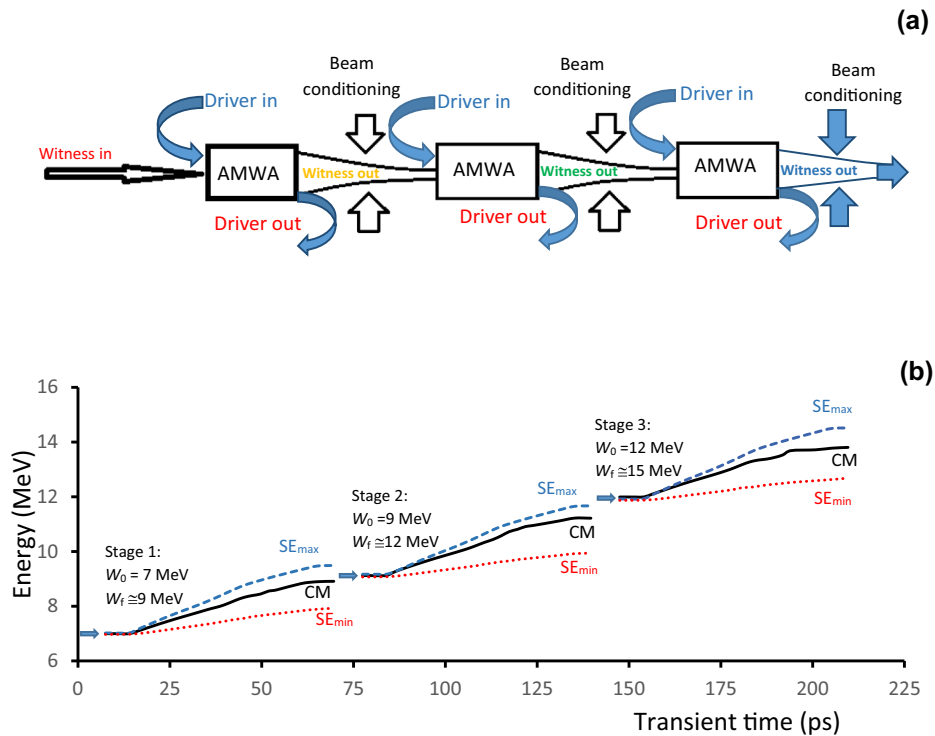


FIG. 5. (a) Schematic illustration of the AMWA cascade accelerator. (b) Results of numerical simulations using 3D PiC code *MAGIC*. An example of acceleration of the witness bunch from 7 MeV (CM) to above 14 MeV (CM) in three stages. Figure 5(b) is to illustrate two main challenges in the realization of the AMWA cascade accelerator concept: driver depletion (needs for three sections) and witness bunch energy spread at the exit of the AMWA section. The dependences of the WB energies on the bunch transient time in stages are shown by the top dashed line (SE_{max}—maximum energy), solid line (CM), dotted line (SE_{min}—minimum energy).

periodic surface lattice have been carried out, it has been demonstrated that an accelerating field gradient up to 1 GeV/m can be achieved and preliminary results demonstrating the concept of a “cascade all-metal wakefield accelerator” have been presented. In this work, the key challenges have been identified, including the energy spread of the witness bunch and the depletion of the driver due to charge loss and radial beam dispersion. In particular, it has been shown that the electrons in the bunch gain radial momentum due to the pondermotive force $\vec{F} = -\left(\frac{e^2}{4m_0\omega_d^2}\right)\vec{\nabla}\left(\frac{E(r)^2}{\gamma(r)}\right)$ and that the bunch spreads radially in the positive (toward the metal surface) and negative (toward the axis of the cylindrical structure) directions. It has been suggested that some of these issues can be overcome by optimizing the geometry of the surface periodic structure and by introducing an external magnetic field to focus the beam and reduce the pondermotive forces.

In this work, several important factors have been analyzed and considered in this paper including the dependence of the wakefield amplitude and the electron dispersion of the driver bunch and electron beam loss on the bunch grating separation; the dependence of the acceleration of the witness bunch in the driver-witness pair separation while demonstrating a shift from the accelerating phase to the decelerating phase when the driver-witness

separation becomes larger as compared with the width of the accelerating bucket. The witness bunch energy spread on the witness bunch length has been investigated. Results show that increasing the length of the witness bunch initially increases the energy spread of the electrons up to a certain length, at which point the amplitude of the energy spread saturates. The results confirmed expectations from previous work and demonstrated the potential to generate a wakefield similar to that observed in a conventional, dielectric wakefield accelerating structure by constructing an “all-metal wakefield accelerator” based on a 2D surface structure. There are clear benefits in being able to eliminate the dielectric material including improved longevity of the system and better thermal and static charge management. The results observed will be used to plan, carry out, and analyze the possible future experiments, which are currently discussed at the University of Strathclyde [40].

ACKNOWLEDGMENTS

I would like to thank Science and Technology Facilities Council (STFC), United Kingdom, for partial support via a grant (The John Adam's Institute for Accelerator Science, ST/P002048/1). I would also like to thank Sevastopol State University for partial support of the work via an internal grant (42-01-09/169/2021-3). I would like to thank

Professor A. D. R. Phelps and Dr. A. J. MacLachlan for useful discussions and encouragement.

-
- [1] A. Novokhatski, Wakefield potentials of corrugated structures, *Phys. Rev. ST Accel. Beams* **18**, 104402 (2015); K. L. F. Bane and G. Stupakov, Using surface impedance for calculating wakefields in flat geometry, *Phys. Rev. ST Accel. Beams* **18**, 034401 (2015).
- [2] P. Emma, M. Venturini, K. Bane *et al.*, Experimental Demonstration of Energy-Chirp Control in Relativistic Electron Bunches Using a Corrugated Pipe., *Phys. Rev. Lett.* **112**, 034801 (2014).
- [3] D. Wang, S. Antipov, C. Jing, J. G. Power, M. Conde, E. Wisniewski, W. Liu, J. Qiu, G. Ha, V. Dolgashev, C. Tang, and W. Gai, Interaction of an Ultrarelativistic Electron Bunch Train with a W-Band Accelerating Structure: High Power and High Gradient, *Phys. Rev. Lett.* **116**, 054801 (2016); X. Lu, M. A. Shapiro, and R. J. Temkin, Novel metallic structures for wakefield acceleration, in *Proceedings of the 3rd North American Particle Accelerator Conference, NAPAC2016, Chicago, IL (JACoW, Geneva, Switzerland, 2016)*, WEPOA33, pp. 762–764, ISBN 978-3-95450-180-9, <https://accelconf.web.cern.ch/napac2016/papers/wepoa33.pdf>.
- [4] F. C. Fu, R. Wang, and P. F. Zhu, Demonstration of Nonlinear-Energy-Spread Compensation in Relativistic Electron Bunches with Corrugated Structures, *Phys. Rev. Lett.* **114**, 114801 (2015).
- [5] V. Blackmore, G. Doucas, C. Perry, B. Ottewell, M. Kimmitt, M. Woods, S. Molloy, and R. Arnold, First measurements of the longitudinal bunch profile of a 28.5 GeV beam using coherent Smith-Purcell radiation, *Phys. Rev. ST Accel. Beams* **12**, 032803 (2009).
- [6] I. V. Konoplev, L. Fisher, A. W. Cross, A. D. R. Phelps, K. Ronald, and M. Thumm, Excitation of surface field cavity and coherence of electromagnetic field scattering on two-dimensional cylindrical lattice, *Appl. Phys. Lett.* **97**, 261102 (2010); I. V. Konoplev, A. W. Cross, P. MacInnes, W. He, A. D. R. Phelps, C. G. Whyte, K. Ronald, and C. W. Robertson, Free-electron maser based on a cavity with two- and one-dimensional distributed feedback, *Appl. Phys. Lett.* **92**, 211501 (2008).
- [7] H. Zhang, I. V. Konoplev, G. Doucas, and J. Smith, Concept of a tunable source of coherent THz radiation driven by a plasma modulated electron beam, *Phys. Plasmas* **25**, 043111 (2018).
- [8] G. Burt, S. V. Samsonov, K. Ronald *et al.*, Dispersion of helically corrugated waveguides: Analytical, numerical, and experimental study, *Phys. Rev. E* **70**, 046402 (2004).
- [9] G. G. Denisov, V. L. Bratman, A. W. Cross, W. He, A. D. R. Phelps, K. Ronald, S. V. Samsonov, and C. G. Whyte, Gyrotron Traveling Wave Amplifier with a Helical Interaction Waveguide, *Phys. Rev. Lett.* **81**, 5680 (1998).
- [10] M. Mineo and C. Paoloni, Double-corrugated rectangular waveguide slow-wave structure for terahertz vacuum devices, *IEEE Trans. Electron Devices* **57**, 3169 (2010).
- [11] C. Paoloni, D. Gamzina, R. Letizia, Y. Zheng, and N. C. Luhmann, Jr., Millimeter wave traveling wave tubes for the 21st century, *J. Electromagn. Waves Appl.* **35**, 567 (2021).
- [12] H. L. Andrews, F. Bakkali Taheri, J. Barros *et al.*, Longitudinal profile monitors using coherent Smith–Purcell radiation, *Nucl. Instrum. Methods Phys. Res., Sect. A* **740**, 212 (2014).
- [13] H. Zhang, I. V. Konoplev, A. J. Lancaster, H. Harrison, G. Doucas, A. Aryshev, M. Shevelev, N. Terunuma, and J. Urakawa, Non-destructive measurement and monitoring of separation of charged particle micro-bunches, *Appl. Phys. Lett.* **111**, 043505 (2017).
- [14] Y. Liang, Y. Du, X. Su *et al.*, Observation of coherent Smith-Purcell and transition radiation driven by single bunch and micro-bunched electron beams, *Appl. Phys. Lett.* **112**, 053501 (2018).
- [15] I. V. Konoplev, G. Doucas, H. Harrison, A. J. Lancaster, and H. Zhang, Single shot, nondestructive monitor for longitudinal subpicosecond bunch profile measurements with femtosecond resolution, *Phys. Rev. Accel. Beams* **24**, 022801 (2021).
- [16] A. J. MacLachlan, C. W. Robertson, I. V. Konoplev, A. W. Cross, A. D. R. Phelps, and K. Ronald, Resonant Excitation of Volume and Surface Fields on Complex Electrodynamic Surfaces, *Phys. Rev. Appl.* **11**, 034034 (2019).
- [17] K. Lekomtsev, A. Lyapin, S. T. Boogert, P. V. Karataev, J. S. Adams *et al.*, Drive-witness acceleration scheme based on corrugated dielectric mm-scale capillary, in *Proceedings of the 8th International Particle Accelerator Conference, IPAC2017, Copenhagen, Denmark (JACoW, Geneva, Switzerland, 2017)* pp. 3292–3295; K. Lekomtsev, A. Aryshev, A. A. Tishchenko, M. Shevelev, A. A. Ponomarenko, P. Karataev *et al.*, Sub-THz radiation from dielectric capillaries with reflectors, *Nucl. Instrum. Methods Phys. Res., Sect. B* **402**, 148 (2017).
- [18] I. V. Konoplev, D. W. Posthuma De Boer, C. M. Warsop, and M. John, Design and characterisation of frequency selective conductive materials for electromagnetic fields control, *Sci. Rep.* **10**, 19351 (2020).
- [19] S. Antipov, C. Jing, M. Fedurin, W. Gai, A. Kanareykin, K. Kusche, P. Schoessow, V. Yakimenko, and A. Zholents, Experimental Observation of Energy Modulation in Electron Beams Passing through Terahertz Dielectric Wakefield Structures, *Phys. Rev. Lett.* **108**, 144801 (2012); S. Antipov, S. Baturin, C. Jing, M. Fedurin, A. Kanareykin, C. Swinson, P. Schoessow, W. Gai, and A. Zholents, Experimental Demonstration of Energy-Chirp Compensation by a Tunable Dielectric-Based Structure, *Phys. Rev. Lett.* **112**, 114801 (2014).
- [20] I. V. Konoplev, A. J. MacLachlan, C. W. Robertson, A. W. Cross, and A. D. R. Phelps, Cylindrical periodic surface lattice as a metadielectric: Concept of a surface-field Cherenkov source of coherent radiation, *Phys. Rev. A* **84**, 013826 (2011).
- [21] I. V. Konoplev, A. D. R. Phelps, A. W. Cross, and K. Ronald, Experimental studies of the influence of distributed power losses on the transparency of two-dimensional surface photonic band-gap structures, *Phys. Rev. E* **68**, 066613 (2003); I. V. Konoplev, A. R. Phipps, A. D. R. Phelps, C. W. Robertson, K. Ronald, and A. W. Cross,

- Surface field excitation by an obliquely incident wave, *Appl. Phys. Lett.* **102**, 141106 (2013).
- [22] A. V. Arzhannikov, A. W. Cross, N. S. Ginzburg, W. He, P. V. Kalinin *et al.*, Production of powerful spatially coherent radiation in planar and coaxial FEM exploiting two-dimensional distributed feedback, *IEEE Trans. Plasma Sci.* **37**, 1792 (2009).
- [23] M. Thompson, H. Badakov, A. Cook, J. Rosenzweig, R. Tikhoplav, G. Travish, I. Blumenfeld, M. Hogan, R. Ischebeck, N. Kirby *et al.*, Breakdown Limits on Gigavolt-per-Meter Electron-Beam-Driven Wakefields in Dielectric Structures, *Phys. Rev. Lett.* **100**, 214801 (2008).
- [24] B. D. O'Shea *et al.*, Observation of acceleration and deceleration in giga-electron-volt-per-metre gradient dielectric wakefield accelerators, *Nat. Commun.* **7**, 12763 (2016).
- [25] G. Andonian *et al.*, Planar-Dielectric-Wakefield Accelerator Structure Using Bragg-Reflector Boundaries, *Phys. Rev. Lett.* **113**, 264801 (2014).
- [26] M. I. Ivanyan, L. V. Aslyan, K. Floettmann, F. Lemery, and V. M. Tsakanov, Wake fields in conducting waveguides with a lossy dielectric channel, *Phys. Rev. Accel. Beams* **23**, 041301 (2020).
- [27] G. Burt, R. Letizia, C. Paoloni, S. P. Jamison, Y. Saveliev, R. B. Appleby, D. M. Graham, T. H. Pacey, H. Owen, G. Xia, A. W. Cross, A. Phelps, and K. Ronald, Dielectric and THz acceleration (data) programme at the Cockcroft institute. in *Proceedings of 28th Linear Accelerator Conference (LINAC2016)*, East Lansing, MI, 2016 (JACoW, Geneva, Switzerland, 2016), pp. 62–64, <http://epaper.kek.jp/linac2016/papers/proceed.pdf>.
- [28] A. M. Cook, S. Y. Tochitsky, R. Tikhoplav, G. Travish, O. B. Williams, and J. B. Rosenzweig, Observation of Narrow-Band Terahertz Coherent Cherenkov Radiation from a Cylindrical Dielectric-Lined Waveguide, *Phys. Rev. Lett.* **103**, 095003 (2009).
- [29] I. V. Konoplev and A. D. R. Phelps, High-gain Compton free electron laser driven by pre-bunched electrons, *Phys. Plasmas* **7**, 4280 (2000).
- [30] A. W. Cross, I. V. Konoplev, A. D. R. Phelps, and K. Ronald, Studies of surface two-dimensional photonic band-gap structures, *J. Appl. Phys.* **93**, 2208 (2003).
- [31] I. V. Konoplev, A. W. Cross, and A. D. R. Phelps, Relativistic electron beam excitation of surface fields in artificial materials based on one- and two-dimensional periodic structures, *IEEE Trans. Plasma Sci.* **39**, 2610 (2011).
- [32] C. L. Holloway, E. F. Kuester, J. A. Gordon, John O'Hara, Jim Booth, and David R. Smith, An overview of the theory and applications of metasurfaces: The two-dimensional equivalents of metamaterials, *IEEE Antennas Propag. Mag.* **54**, 10 (2012).
- [33] S. A. Tretyakov, Metasurfaces for general transformations of electromagnetic fields., *Philos. Trans. R. Soc. A* **373**, 20140362 (2015).
- [34] A. J. MacLachlan, C. W. Robertson, A. W. Cross, and A. D. R. Phelps, Volume and surface mode coupling experiments in periodic surface structures for use in mm-THz high power radiation sources., *AIP Adv.* **8**, 105115 (2018).
- [35] A. V. Kildishev, A. Boltasseva, and V. M. Shalaev, Planar photonics with metasurfaces, *Science* **339**, 1232009 (2013); E. Nanni, W. Huang, K. H. Hong, Koustuban Ravi, Arya Fallahi, Gustavo Moriena, R. J. Dwayne Miller, and Franz X. Kärtner Terahertz-driven linear electron acceleration, *Nat. Commun.* **6**, 8486 (2015).
- [36] I. V. Konoplev, L. Fisher, A. W. Cross, A. D. R. Phelps, K. Ronald, and M. Thumm, Excitation of surface field cavity and coherence of electromagnetic field scattering on two-dimensional cylindrical lattice, *Appl. Phys. Lett.* **97**, 261102 (2010).
- [37] I. V. Konoplev, A. D. R. Phelps, A. W. Cross, and K. Ronald, Experimental studies of the influence of distributed power losses on the transparency of two-dimensional surface photonic band-gap structures, *Phys. Rev. E* **68**, 066613 (2003).
- [38] A. R. Phipps, A. J. MacLachlan, C. W. Robertson, L. Zhang, I. V. Konoplev, A. W. Cross, and A. D. R. Phelps, Electron beam excitation of coherent sub-terahertz radiation in periodic structures manufactured by 3D printing, *Nucl. Instrum. Methods Phys. Res., Sect. B* **402**, 202 (2017).
- [39] Y. Saveliev, T. J. Overton, T. H. Pacey, N. Joshi, S. Mathisen, B. D. Muratori, N. Thompson, M. P. King, and G. Xia, Experimental study of transverse effects in planar dielectric wakefield accelerating structures with elliptical beams, *Phys. Rev. Accel. Beams* **25**, 081302 (2022).
- [40] A. D. R. Phelps and A. W. Cross (private communication).